

Serveur Académique Lausannois SERVAL serval.unil.ch

Author Manuscript

Faculty of Biology and Medicine Publication

This paper has been peer-reviewed but does not include the final publisher proof-corrections or journal pagination.

Published in final edited form as:

Title: Deletion of the RNA-binding proteins ZFP36L1 and ZFP36L2 leads to perturbed thymic development and T lymphoblastic leukemia.

Authors: Hodson DJ, Janas ML, Galloway A, Bell SE, Andrews S, Li CM, Pannell R, Siebel CW, MacDonald HR, De Keersmaecker K, Ferrando AA, Grutz G, Turner M

Journal: Nature immunology

Year: 2010 Aug

Volume: 11

Issue: 8

Pages: 717-24

DOI: 10.1038/ni.1901

In the absence of a copyright statement, users should assume that standard copyright protection applies, unless the article contains an explicit statement to the contrary. In case of doubt, contact the journal publisher to verify the copyright status of an article.

Published in final edited form as:

Nat Immunol. 2010 August ; 11(8): 717–724. doi:10.1038/ni.1901.

Deletion of the RNA-binding proteins *Zfp36l1* and *Zfp36l2* leads to perturbed thymic development and T-lymphoblastic leukaemia

Daniel J. Hodson¹, Michelle L. Janas¹, Alison Galloway¹, Sarah E. Bell¹, Simon Andrews², Cheuk M. Li¹, Richard Pannell³, Christian W. Siebel⁴, H. Robson MacDonald⁵, Kim De Keersmaecker⁶, Adolfo A. Ferrando^{6,7,8}, Gerald Grutz^{9,10}, and Martin Turner¹

¹Laboratory of Lymphocyte Signalling and Development, The Babraham, Cambridge, CB22 3AT, United Kingdom ²Bioinformatics Group, The Babraham Institute, Babraham, Cambridge, CB22 3AT, United Kingdom ³MRC Laboratory of Molecular Biology, Hills Road, Cambridge CB2 0QH, UK ⁴Genentech, Department of Molecular Biology, 1 DNA Way, South San Francisco, CA 94080 USA ⁵Ludwig Institute for Cancer Research, Lausanne Branch, University of Lausanne, 1066 Epalinges, Switzerland ⁶Institute for Cancer Genetics, Columbia University Medical Centre, New York, USA ⁷Department of Pathology, Columbia University Medical Centre, New York, USA ⁸Department of Pediatrics, Columbia University Medical Centre, New York, USA ⁹Institute of Medical Immunology, Charité-Universitätsmedizin, Campus Mitte, Berlin, Germany ¹⁰Center for Biomaterial Development, Institute of Polymer Research, GKSS, Teltow, Germany

Abstract

ZFP36L1 and ZFP36L2 are RNA-binding proteins (RBPs) which interact with AU-rich elements in the 3'UTR of mRNA, leading to mRNA degradation and translational repression. Mice lacking ZFP36L1 and ZFP36L2 during thymopoiesis develop a Notch1-dependent T cell acute lymphoblastic leukaemia (T-ALL). Prior to the onset of T-ALL, thymic development is perturbed with accumulation of cells which have passed through the β -selection checkpoint without first expressing T cell receptor β (TCR- β). Notch1 expression is increased in non-transformed thymocytes in the absence of ZFP36L1 and ZFP36L2. Both RBPs interact with evolutionarily conserved AU-rich elements within the 3' untranslated region of Notch1 and suppress its expression. These data establish a role for ZFP36L1 and ZFP36L2 during thymocyte development and in the prevention of malignant transformation.

The development of T cells in the thymus proceeds through a series of developmental stages characterised by progressive rearrangement of the T cell receptor (TCR) genes and regulated by a series of developmental checkpoints. This ordered process is orchestrated by transcription factor networks which integrate environmental cues to initiate gene expression programs appropriate to the developmental stage of the thymocyte^{1–3}. However there is increasing recognition that gene expression during lymphocyte development is also subject to regulation by post-transcriptional mechanisms. These affect the half-life of mRNA through promotion or

*Correspondence should be addressed to M.T. (martin.turner@bbsrc.ac.uk). Laboratory of Lymphocyte Signalling and Development, The Babraham Institute, Babraham, Cambridge CB22 3AT, United Kingdom. tel +44 (0)1223 496403. fax +44(0)1223 496023.

AUTHOR CONTRIBUTIONS D.J.H. designed and performed experiments, analysed data and wrote the paper; M.J., A.G., S.E.B., designed and performed experiments; C.M.L., R.P., G.G., C.W.S. and H.R.M. developed analytical tools; S.A. designed experiments, analysed data; M.T. designed experiments, analysed data and wrote the paper.

Accession codes: Microarray data has been submitted to the European Bioinformatics Institute ArrayExpress database, accession number E-MEXP-2737.

COMPETING INTERESTS STATEMENT C.W.S. was employed by Genentech Inc. during the course of this study.

inhibition of mRNA decay. Additional control at the point of mRNA translation also regulates the magnitude of gene expression. These points are exemplified by recent awareness of the regulation of gene expression by microRNAs which act principally through the control of mRNA decay and translation. Post-transcriptional control of gene expression is also mediated by RNA-binding proteins (RBPs) of which over 150 have been found to be expressed in thymus⁴. However, our knowledge of how post-transcriptional regulation mediated by RNA-binding proteins impacts on thymic development is extremely limited.

ZFP36L1 and ZFP36L2 (also known as TIS11b and TIS11d) belong to a family of CCCH-zinc finger-containing RBPs that includes ZFP36 (tristetraprolin). These regulate gene expression by promoting mRNA decay and might additionally affect translation. A germline *Zfp36* knockout mouse develops a severe inflammatory phenotype attributable to overexpression of TNF⁵⁻⁶ while germline knockout of *Zfp36l1* is lethal at embryonic day 10.5 due to a failure of chorioallantoic fusion⁷⁻⁸. Germline *Zfp36l1* knockout mice die shortly after birth possibly as a consequence of haematopoietic stem cell failure⁹. The tandem zinc fingers are highly conserved between TTP family members and bind to AU-rich elements (ARE) in the 3'-untranslated region (3'UTR) of mRNA, promoting deadenylation and decay. The optimum binding sequence for all family members is UUAUUUAU¹⁰⁻¹¹. However sequences as short as UAUUU may be sufficient for binding and genome-wide screens to identify targets have been enriched with transcripts that do not possess the optimal AU-rich binding site¹². Thus the criteria for target recognition, and whether this differs between the family members, remain incompletely defined.

There is mounting evidence that escape from post-transcriptional regulation of gene expression is important in the pathogenesis of malignancy. Deletion of the miR15a & miR16-1 cluster in mice leads to development of a disease similar to human chronic lymphocytic leukaemia¹³. Aberrant polyadenylation site usage, leading to a truncated 3'UTR, has been detected in many human malignancies and might allow malignant cells to escape regulation by both microRNA and RBPs¹⁴⁻¹⁵. As a physiological mechanism, proliferating T cells preferentially utilise truncated 3'UTRs¹⁶. This is consistent with a global reduction in post-transcriptional regulation providing a net proliferative advantage. Circumstantial evidence implicates ZFP36 family members in malignancy. Expression of ZFP36 is suppressed in a variety of human malignancies¹⁷. ZFP36L2 has been suggested to act downstream of p53 in the induction of apoptosis and ZFP36L1 is implicated in the apoptotic response to rituximab (anti-CD20) in chronic lymphocytic leukaemia¹⁸⁻¹⁹. A number of oncogenes, including *FOS*, *MYC*, *BCL-2*, and *COX-2* contain AREs in their 3'UTRs and have been proposed as potential targets²⁰. However no evidence to date proves an *in vivo*, physiological tumor suppressor role for ZFP36 family members, or indeed any RBP.

To investigate the function of ZFP36L1 and ZFP36L2 in thymic development we generated conditional knockouts of both genes. In anticipation of redundancy between these two closely related family members we inter-crossed the single knockouts to create lymphocyte conditional *Zfp36l1* and *Zfp36l2* double knockout (dKO) mice. Thymic development was normal in the single knockouts, however the dKO mice developed T-lymphoblastic leukaemia T-ALL). Prior to leukaemia the normally ordered process of thymic development was perturbed, with aberrant passage of thymocytes through the β -selection checkpoint. Furthermore the oncogenic transcription factor *Notch1* was identified as a novel target of ZFP36L1 and ZFP36L2. The finding that a transcription factor is itself a target for post-transcriptional regulation, demonstrates how RBPs integrate gene expression at the transcriptional and post-transcriptional level. These findings identify a critical role for ZFP36 family members during lymphocyte development and provide the strongest evidence to date for their function as tumor suppressors.

Results

Double knockout mice develop T-ALL

Zfp3611 and *Zfp3612* are expressed throughout thymic development, especially during the early CD4⁻CD8⁻ double negative stages (Supplementary Fig. 1). To examine their function conditional knockout mice were generated using standard gene targeting techniques (Supplementary Fig. 2). Mice were inter-crossed and bred to homozygosity for the floxed alleles of both *Zfp3611* and *Zfp3612*. Transgenic expression of Cre under the control of a *CD2* locus control region was used to effect deletion prior to the double negative 1 (DN1) stage of thymic development^{21–22}. Unless otherwise stated control mice were *Zfp3611*^{fl/fl}*Zfp3612*^{fl/fl}. We confirmed that the expression of the *CD2-Cre* transgene alone caused no associated defect in thymic development (data not shown).

Zfp3611^{fl/fl}*Zfp3612*^{fl/fl}*CD2Cre* mice, hereafter referred to as double knockout (dKO) for simplicity, were born at expected Mendelian ratios and appeared healthy in early life. However, 90% of dKO mice died or were humanely culled due to ill health by six-months of age (Fig. 1a). All of these mice had developed thymic tumors and many also showed splenomegaly and lymphadenopathy (Supplementary Fig. 3). Tumor development was never observed in *Zfp3611*^{fl/fl}*CD2-Cre* or *Zfp3612*^{fl/fl}*CD2-Cre* single mutant mice, or in any intermediate combination of genotypes (e.g. *Zfp3611*^{fl/fl}*Zfp3612*^{fl/+}*CD2-Cre*). Thus a single allele of either *Zfp3611* or *Zfp3612* appeared sufficient to prevent tumor development. All thymic tumors showed high CD8 expression, with variable CD4 expression (Fig. 1b). Tumor cells expressed high amounts of heat stable antigen (CD24) but did not express surface T cell receptor beta (sTCR-β). Most, but not all tumors, expressed intracellular TCR-β (icTCR-β). Circulating lymphoblasts were seen upon examination of the peripheral blood (Fig. 1c,d). Flow cytometric analysis of spleen, lymph node and bone marrow frequently demonstrated involvement by tumor cells of identical phenotype to the associated thymic tumor (Fig 1e). Clonality testing by PCR across the TCR-β2 region suggested that thymic tumors were predominantly oligoclonal (Fig. 1f). Taken together, these findings suggest that deletion of *Zfp3611* and *Zfp3612* together leads to the development of T-ALL corresponding to the CD8 immature single positive (CD8iSP) and double positive (DP) stages of thymic development.

Perturbed thymopoiesis prior to tumor development

In dKO mice, tumor development was preceded by thymic atrophy. At three and eight weeks of age total thymic cellularity was approximately 50% that of control mice (Fig. 2a,b). This atrophic stage was associated with the gradual expansion of the CD8iSP population (CD8⁺CD4⁻CD24^{hi}sTCRβ⁻). By thirteen weeks this population was markedly expanded in both proportion and absolute number (Fig. 2c,d). Abnormal development was also observed at the CD4⁻CD8⁻ (DN) stages (Fig. 2e). The expression of CD44 and CD25 are used to describe four stages of DN development and appeared to show a reduced progression from DN2 (CD44⁺CD25⁺) to DN3 (CD44⁻CD25⁺) (Fig. 2e). However the utility of this staining strategy to describe functional progression in the face of perturbed thymic development is limited. Therefore, we examined the expression of intra-cellular TCR-β (icTCR-β) which normally becomes expressed during the DN3 stage following successful TCR-β rearrangement. In dKO mice the proportion of DN thymocytes expressing icTCR-β was markedly reduced (Fig. 2e & Supplementary Fig. 4). In wild-type mice the expression of icTCR-β is a prerequisite for cells to pass the β-selection checkpoint. However in dKO mice these icTCR-β⁻ cells displayed features of metabolic activation normally only seen following β-selection. The expression of the amino acid transporter CD98 and the transferrin receptor CD71 is normally low prior to β-selection but increases in a Notch1-dependent manner following β-selection as cellular metabolism increases²³. However expression of CD98 and CD71 was high in all DN thymocytes from dKO mice suggesting metabolic activation even in icTCR-β⁻ thymocytes. (Fig. 2e). Consistent with this, icTCR-β⁻ dKO cells showed elevated forward scatter typical

of blasting cells (data not shown). Furthermore, cellular proliferation was elevated, as judged by increased uptake of EdU following pulse administration (Supplementary Fig. 5). Thus it appeared that dKO thymocytes were able to transit the β -selection checkpoint, with associated metabolic activation and proliferation, but without expression of TCR- β . This aberrant passage through β -selection was associated with differentiation of icTCR β^- thymocytes to the CD8iSP and DP developmental stages which lie downstream of β -selection. As expected, in control mice all thymocytes from the CD8iSP and DP stages expressed icTCR- β . However, in dKO thymocytes, icTCR- β was expressed by only 30% of CD8iSP (Fig. 2e & Supplementary Fig. 4). This increased to 90% of DP and 100% at the CD4 and CD8 mature single positive (CD8mSP) stages (Supplementary Fig. 4). Thus although dKO icTCR- β^- cells were able to pass β -selection they were unable to progress beyond the DP stage. Despite the accumulation of TCR β^- CD8iSPs, the majority of thymic tumors corresponded to TCR β^+ CD8iSP thymocytes suggesting the importance of preTCR signals during leukaemia development.

Elevated Notch1 expression in dKO thymocytes

We hypothesised that the thymic phenotype observed in dKO mice might result from the over-expression of one or more genes normally suppressed by ZFP36L1 or ZFP36L2. We performed microarray analysis upon whole thymus from control and dKO mice, aged five weeks old and nine weeks old, as this was prior to the development of tumor and, at five weeks of age, the relative thymic proportions were normal, as judged by CD4 and CD8 staining (Fig. 1a). At nine weeks of age more than 500 significantly changing genes were elevated more than 1.5 fold. Fewer were elevated at five weeks. When the list was filtered to include only genes elevated in both the five week and the nine week arrays, 17 named genes were identified (Fig. 3a). Of these 17 up-regulated genes, we chose to investigate further the expression of *Notch1* as this gene is critical for thymic development and in the pathogenesis of T-ALL²⁴. Elevation of mRNA encoding Notch1 and its target genes, *Hes1*, *Myc* and *Dtx1*, was confirmed by real time PCR (Fig. 3b). We also showed strong expression of Notch1 protein in thymic tumors, both by immunoblot and flow cytometry (Fig. 3c,d). Notch1 expression by flow cytometry was between 5- and 50-fold higher in thymic tumor than in control thymus (Fig. 3d). Notch1 staining was higher in thymic tumor than any individual subpopulation of control thymus suggesting that the elevated tumor expression did not merely reflect an expansion of immature populations (Fig. 3e). We also examined Notch1 expression in individual thymic subsets in mice prior to the development of tumor. In mice aged three weeks old, Notch1 expression was elevated at the DN stages. Elevated Notch1 expression was seen in both CD25⁺icTCR- β^- and in CD25⁺icTCR- β^- DN thymocytes (Fig. 3f). Elevated Notch1 expression was also seen at the CD8iSP stage. In dKO mice, both icTCR- β^+ and icTCR- β^- CD8iSP populations highly expressed Notch1 (Fig. 3g). Thus Notch1 was abnormally elevated in both DN and CD8iSP thymocytes from dKO mice prior to the onset of T-ALL. This high expression of Notch1 is increased even further in dKO tumor cells.

Notch1 is a target of ZFP36L1 and ZFP36L2

The 1.6Kb *Notch1* 3'UTR contains a region of particularly high interspecies conservation within the 300bp following the translation termination codon (Fig. 4a). Within this highly conserved region (HCR), the greatest interspecies conservation is clustered into three short regions. Strikingly each of these contains a predicted ZFP36L1 and ZFP36L2 binding site (Fig. 4b). These binding sites are not found elsewhere in the *Notch1* 3'UTR. When we examined the 3'UTRs of all 17 genes up-regulated in the microarray, *Notch1* was the only gene to contain the nonameric ARE considered to be the optimum binding site for ZFP36L1 and ZFP36L2. To determine whether the *Notch1* 3'UTR could mediate suppression by ZFP36L1 or ZFP36L2 we introduced the complete *Notch1* 3'UTR downstream of the luciferase coding region in pSI-Check2. When this reporter was transfected into HEK293T cells (which do not constitutively express *Zfp36l1* or *Zfp36l2*) the co-transfection of either *Zfp36l1* or *Zfp36l2* suppressed

luciferase activity in a dose dependent manner (Fig. 4c and d). This effect required functional RNA-binding zinc fingers of *Zfp361l*, as a mutant version of *Zfp361l* in which both fingers were mutated and which could no longer bind RNA, failed to suppress the *Notch1* UTR reporter (Fig. 4c). Furthermore, a reporter containing only the HCR was suppressed by *Zfp361l* and *Zfp3612* but these had no effect upon a reporter containing the remainder of the UTR lacking the HCR. In all of these assays expression of ZFP36L1, ZFP36L2 and tandem zinc finger mutant (TZFM) was confirmed by immunoblot (data not shown). To demonstrate a direct physical interaction between ZFP36L1 or ZFP36L2 and the *Notch1* 3'UTR we used a radiolabelled probe (corresponding to 61 nucleotides of the *Notch1* 3'UTR containing the nonameric binding site) in an electromobility shift assay (EMSA). Lysate from HEK293T cells transfected with empty pCDNA3 or with pCDNA3-ZFP36L1-TZFM expression vector failed to retard the migration of the probe. By contrast, lysates from pCDNA3-ZFP36L1, or pCMV2-ZFP36L2 transfected cells yielded a probe complex with retarded mobility indicative of a direct interaction (Fig. 4e). The size of these complexes correlated with the molecular weight of ZFP36L1 (36kDa) and ZFP36L2 (50kDa).

Taken together these results indicate a direct interaction between ZFP36L1 and ZFP36L2 with the HCR of the *Notch1* 3'UTR and that this interaction mediates a suppressive effect upon gene expression.

Infrequent Notch1 mutation in dKO mutant tumors

Mutation of the PEST domain of *NOTCH1* is frequently found in human and mouse models of T-ALL and renders Notch1 protein resistant to degradation. Mutation of the heterodimerisation (HD) domain is also observed and leads to spontaneous cleavage of Notch1 leading to ligand independent signaling activity²⁵. We consider it likely that the absence of ZFP36L1 and ZFP36L2 explains the elevation of Notch1 observed in thymocytes prior to the development of leukaemia. However the oligoclonal nature of the tumors suggests a second hit – possibly leading to activation of an already over-expressed Notch1 receptor. To examine this possibility we sequenced the PEST and HD domains of *Notch1* in thymic tumors from 12 dKO mice. One PEST domain mutation was detected (insertion C at amino acid position 2421 leading to frame-shift and premature stop). Three HD mutations, reported previously in both human and mouse T-ALL, were found (all T to C in residue 1668) which result in a leucine to proline switch²⁵. Thus *Notch1* mutation was found in a minority of tumors and predominantly affected the HD (25%) rather than the PEST domain (8%).

Tumors are Notch1-dependent and killed by ZFP36L1 re-expression

To establish if tumors were Notch-dependent we cultured primary tumor cells from dKO mice on OP9-DL1 stromal cells in the presence of increasing concentrations of the gamma-secretase inhibitor compound E which inhibits Notch signaling. After 72 hours cells were counted and analysed by flow cytometry (Fig. 5a). Tumor growth was clearly sensitive to compound E which was effective at concentrations as low as 0.1 μ M. To establish if tumor development was Notch1-dependent *in vivo* we treated 12-week old mice with a Notch1 blocking antibody or saline control. This antibody is directed against the extracellular negative regulatory region of Notch1 and stabilises its inactive state²⁶. In control mice receiving the Notch1 blocking antibody thymic cellularity was reduced to <1% of normal and this consisted predominantly of mature CD4 and CD8 single positive cells (Fig. 5b,c). This demonstrated the ability of the antibody to block Notch1 signaling. Of the dKO mice receiving saline injections, thymic tumors were seen in two (20%) and all showed grossly abnormal thymic populations by flow cytometry (Fig. 5c). No tumors were seen in dKO mice receiving the Notch1 blocking antibody and most had thymic cellularity <1% of normal. Two mice in this cohort had an apparently enlarged thymus that consisted of predominantly necrotic cells. We consider it likely that these represent pre-existing thymic tumors that were killed by Notch1 blockade. Notch1 antibody

treatment also led to the disappearance of CD8⁺CD4⁻CD24^{hi}TCR-β⁻ and the CD8⁺CD4⁻CD24^{hi}TCR-β⁺ populations in the dKO mice (Fig. 5c) indicating the expansion or maintenance of these cells *in vivo* was Notch1 dependent.

To establish the effect of re-expression of ZFP36L1 upon tumors cultured *in vitro*, primary tumor cells were cultured on OP9-DL1 and then infected with equivalent titres of retrovirus expressing green fluorescent protein (GFP) and either *ZFP36L1* or the Tandem zinc finger mutant of *ZFP36L1*. Remarkably, ZFP36L1-expressing cells were almost completely depleted from cultures confirming that expression of ZFP36L1 is toxic to primary tumor cells (Fig. 5d). Taken together, these results suggest that the growth and survival of dKO tumor cells remain dependent upon active Notch1 signaling and upon the absence of ZFP36L1.

Discussion

Current models of thymocyte development focus predominantly upon regulation of gene expression at the level of the transcription factor. Recently a role for post-transcriptional regulation of gene expression has been proposed in the context of microRNA²⁷. However post-transcriptional regulation is also mediated by RBPs. To date, our greatest understanding of RBPs has been their ability to regulate the stability of mRNA encoding short-lived cytokines involved in the inflammatory response. Our knowledge of their role during lymphocyte development is limited to a single report describing defective egress of mature thymocytes from the thymus of mice deleted for the RBP *Elavl1*²⁸. Therefore the data presented here establish a novel requirement for ZFP36L1 and ZFP36L2 during normal thymic development. Furthermore they provide clear evidence of a critical role for ZFP36L1 and ZFP36L2 in the prevention of lymphoid malignancy.

Close to 100% of *Zfp36l1-Zfp36l2* dKO mice developed T-ALL, beginning from the age of three months. This phenotype is seen only in dKO mice and never in any intermediate combination of genotypes suggesting a high degree of redundancy between these two highly homologous proteins. The evolutionary need for such redundancy is consistent with the critical role demonstrated here in the prevention of malignancy. The absence of leukaemia from any genotype other than the dKO is evidence against the phenotype being due to an artefact of gene targeting. The toxicity of ZFP36L1, when re-expressed in tumor cells, is further evidence that the leukaemic phenotype does indeed result from the loss of ZFP36L1 and ZFP36L2. The involvement of ZFP36 family members in malignancy has been previously suggested²⁰. Expression of ZFP36 family members is suppressed in a range of human cancers and a tumor suppressor role has been proposed to act through regulation of proliferative and anti-apoptotic factors^{17, 20}. However this is the first example in which the intentional deletion of an RBP leads to the development of malignancy.

Prior to the development of T-ALL, thymic development is perturbed. In particular, thymocytes appear able to bypass β-selection in the absence of a functional TCR-β chain. In *Rag 1* and 2 dKO or TCR-β KO mice, DP differentiation can be partially rescued by deletion of *Izkl1*, *Tcf3* or *Trp53*, or by the transgenic over-expression of *Ras*, *Map2k1* or *Notch1*^{29–32}. However, *Zfp36l1-Zfp36l2* dKO thymocytes are clearly able to recombine the TCR-β chain yet appear to be unable to suppress the developmental progression of TCR-β negative thymocytes. Over-expression of Notch1 in dKO mice might contribute to this aspect of the phenotype. The increased metabolic activity of double negative thymocytes is also consistent with increased expression of Notch1 which is known to promote cellular metabolism in cells at the stage of β-selection³³. Importantly, CD98 and CD71 expression in normal thymocytes is promoted in a Notch1-dependent manner²³. This proves further evidence that, in the absence of both ZFP36L1 and ZFP36L2, Notch1 activity is abnormally elevated in double negative thymocytes.

The over-expression of Notch1, observed prior to and after the development of leukaemia, is also intriguing as chimeric mice reconstituted with bone marrow transduced with retrovirus expressing Notch1-intracellular domain, and other mouse models that overexpress Notch1 invariably develop T-ALL^{24, 34–36}. The observed phenotype of Notch1-driven T-ALL typically corresponds to the CD8iSP and DP stages of thymocyte development and closely resembles the T-ALL seen in *Zfp3611-Zfp3612* dKO mice. The expansion of CD8iSP cells was Notch1-dependent in the dKO mice prior to the onset of T-ALL. The results of luciferase and EMSA experiments suggest that the elevated Notch1 expression is likely to result from alleviation of ZFP36L1 and ZFP36L2-mediated suppression. Regulation of *Notch1* at the post-transcriptional level has been proposed previously in the context of leech development³⁷ but has not been proposed in the context of thymic development. The degree of elevation of Notch1 in dKO mice prior to onset of leukaemia is modest – about two-fold. However we consider this elevation significant because *Notch1* is normally extremely tightly regulated both at the level of transcription and protein stability. The Notch signaling pathway contains no amplification stage, therefore one ligand-receptor engagement leads to one molecule of Notch intracellular domain complexing with a single promoter and activating transcription from a single target allele. Notch1 is also unusual in that a thymic phenotype has been described in the context of haplo-insufficiency³⁸. These factors suggest that the Notch1 signaling pathway has evolved to regulate its expression within very tight limits.

Importantly, overexpression of Notch1 has the capacity to contribute to both the leukaemic phenotype and the aberrant β -selection^{24, 31}. This contribution of Notch1 to the leukaemic phenotype is evidenced by the Notch1-dependency of tumor cells both *in vivo* and *in vitro*. However, it is unclear whether the degree of elevation is, by itself, sufficient to initiate leukaemia formation. The oligoclonal nature of the tumors suggests a “second hit”. This might be mutation of the *Notch1* gene itself leading to the co-operative activation of the Notch1 receptor that is already over-expressed in dKO thymocytes. It is also likely that further unidentified ZFP36L1 and ZFP36L2 targets exist that contribute to the leukemic phenotype. We chose to pursue *Notch1* because of its established role in thymic development and the presence of predicted ZFP36L1 and ZFP36L2 binding sites in the 3'UTR. However ZFP36 family members are promiscuous in their binding requirements and targets might exist that do not possess the classic AU-rich nonamer¹². Furthermore, our microarray experiment would not have detected target genes regulated purely at the level of translation. It is recognised that both microRNA and RBP frequently regulate multiple target mRNA that encode genes with similar functions – so called “RNA regulons”³⁹. Therefore Notch1 might represent one component of a co-ordinated program of gene expression (normally suppressed by ZFP36L1 and ZFP36L2) that regulates the “activation status” of developing thymocytes and, in the absence of ZFP36L1 and ZFP36L2, act together to promote the leukemic phenotype.

While we show here that ZFP36L1 and ZFP36L2 are able to regulate expression of Notch1 it is interesting that *Zfp3612* has previously been identified as a gene positively regulated by Notch1, suggesting that Notch1 induces the expression of its own negative regulator⁴⁰. This is consistent with the mRNA expression pattern of *Zfp3611* and *Zfp3612* which are high during the early DN stages but fall at the DN4 stage concurrent with a fall in Notch1 levels. ZFP36L1 and ZFP36L2 are also regulated post-translationally and their activity is suppressed by phosphorylation, by protein kinase B and by MAPKAP2^{41–43}. There is considerable evidence of interplay between the PI3K and Notch signaling pathways and phosphorylation of ZFP36L1 and ZFP36L2 might provide a further mechanism by which PI3K activity is able to increase Notch1 expression^{44–45}. Both the PI3K and MAP kinase signaling pathways play a crucial role during thymocyte development; in addition to their established roles this could additionally reflect their ability to regulate gene expression at the post-transcriptional level by controlling the activity of RBPs such as ZFP36L1 and ZFP36L2. The instantaneous and reversible manner in which ZFP36L1 and ZFP36L2 activity can be regulated by phosphorylation is well suited

to the changes in gene expression required during thymocyte development. This would provide a mechanism whereby PI3K or MAPK activity could effect rapid changes in expression of transcription factors such as Notch1, thereby integrating extracellular cues with both post-transcriptional and transcriptional control of gene expression.

Our finding that *Notch1* can be regulated at the RNA level is of potentially great significance to human disease. *NOTCH1* is mutated in >50% human T-ALL and co-operating mutations affecting both HD and PEST domains are frequent⁴⁶. Truncation of the 3'UTR as a result of alternative polyadenylation site usage is commonly seen in malignancy and it is plausible that mutation or truncation of the *NOTCH1* 3'UTR might co-operate with coding sequence mutations to further increase NOTCH1 activity. Preliminary experiments involving analysis of array CGH (aCGH) data from 69 human T-ALL samples identified recurrent deletions in chromosome 14q24 including the *ZFP36L1* locus in 3 cases. This finding is intriguing, but of uncertain significance as these were non-focal, heterozygous deletions encompassing several additional genes besides *ZFP36L1*. No genetic alterations involving *ZFP36L2* in chromosome 2 were present in this series. However, many alternative mechanisms might lead to suppression of *ZFP36L1* and *ZFP36L2* activity including epigenetic or post-translational modification by altered kinase or phosphatase activity in leukaemic cells. Similarly, defects downstream of *ZFP36L1* or *ZFP36L2* in the RNA regulation pathway might contribute to the pathogenesis of human malignancy.

In summary, these data reveal a critical role for the RNA-binding proteins *ZFP36L1* and *ZFP36L2* during thymocyte development. They highlight the significant impact of post-transcriptional regulation of gene expression during thymic development. Furthermore, they also demonstrate a critical role for these proteins as tumor suppressors in the prevention of malignant transformation.

Online Methods

Mice

All procedures involving mice were approved by the U.K. Home Office and the Babraham Institute Animal Welfare and Experimentation Committee.

Gene Targeting

The *Zfp36l1* and *Zfp36l2* targeting vectors were generated by inserting LoxP sites either side of exon 2. Correctly targeted embryonic stem cell clones were identified by Southern blotting using both 3' and 5' flanking probes. Chimeras were generated by standard techniques. Mice were bred to FlpE deleter mice to remove the neomycin cassette⁴⁷. Mice were then bred to CD2-Cre transgenic mice. Genotyping was performed using primers listed in Supplementary table 1.

Flow cytometry analysis

Cell suspensions were stained for 30 minutes using antibodies detailed below. For intracellular staining cells were fixed using Cytofix/Cytoperm (BD) and stained for one hour at room temperature in PermWash buffer (BD). FACS data was acquired on an LSRII (BD) and analyzed using FlowJo software (TreeStar).

Flow sorting

Double negative thymic populations were pre-enriched by negative MACS depletion. Cell suspensions were incubated with anti-CD8 biotin, followed by anti-biotin MicroBeads (Miltenyi Biotech) and then applied to MACS separation columns (Miltenyi Biotech). Cells were then stained for CD44, CD25, CD98 and a dump channel (CD4, CD8, TER119, Mac1,

Gr1, B220, NK1.1, $\gamma\delta$ TCR). Cells were sorted on a FACSAria (BD): DN1 (CD44⁺CD25⁻), DN2 (CD44⁺CD25⁺), DN3 (CD44⁻CD25⁺CD98⁻) and DN4 (CD44⁻CD25⁻CD98⁺). CD8 populations were sorted following MACS depletion of CD4 then sorted based on: CD8iSP (CD8⁺sTCR- β ⁻CD24^{hi}) CD8mSP (CD8⁺sTCR- β ⁺CD24^{int}). CD4 and DP populations were sorted by expression of CD4 and CD8.

Antibodies for flow cytometry and immunoblotting

Biotin-Gr1(RB6-8C5), Biotin-NK1.1 (PK136), Biotin- $\gamma\delta$ -TCR (GL3), FITC-CD25 (7D4), PerCP-Cy5.5-CD8 α (53-6.7), PE-CD98 (RL388) and FITC-CD24 (M1/69) were purchased from BD. PE-Cy7-CD4 (L3T4), PECy5.5-CD44 (IM7), PE-CD71 (R17217), PE-TCR- β (H57-597), Biotin-TER119, Biotin-B220 (RA3-6B2) were purchased from eBioscience. Biotin-CD11b (RM2815) was purchased from Caltag. Notch1 staining was performed using PE-Notch1 (mN1A) from BD and Biotin-Notch1 rat IgG2a (22E5.5)⁴⁸. For immunoblotting BRF1/2(#2119) and Cleaved Notch1 (Val1744) (D3B8) were purchased from Cell Signaling Technology. The EdU staining kit was purchased from Invitrogen and used as per the manufacturer's instructions.

Microarray

Samples were prepared from thymus in Trizol (Invitrogen). RNA was extracted using the RNEasy kit (Qiagen) including the on column DNase step. Expression profiling was performed using Affymetrix mouse gene ST1.0 array and analysed using Genespring software. Raw data was subjected to RMA normalisation. Probes whose raw intensity fell into the bottom 20% of every replicate across all conditions were removed as being unexpressed. The remaining probes were tested separately for a significant change in expression between control and either 5 or 9 weeks using an unpaired t-test with a cut-off of $p < 0.05$ after applying a Benjamini and Hochberg multiple testing correction. The significantly changing genes were further filtered to remove any with an absolute change of < 1.5 fold between conditions.

TCR- β 2 Clonality PCR

PCR primers were used as previously described⁴⁹.

RTPCR

cDNA was synthesised from RNA using Superscript II (Invitrogen). RT-PCR was performed using Platinum QPCR mix (Invitrogen) and primers detailed in Supplementary table 1 and run on a Chromo4 analyser (MJ Research). Results were normalised to the reference genes B2M or to GAPDH as indicated in text. See supplementary table 1 for primer sequences. B2M and GAPDH assay were purchased from ABI.

Plasmid Constructs

pcDNA3.myc.WT *ZFP36L1* expression construct and pFLAG.CMV2-*ZFP36L2* were obtained from Dr Andrew Clark (Kennedy Institute of Rheumatology, London). The *ZFP36L1* tandem zinc finger mutant (TZFM) C135/173R was made by site directed mutagenesis. See Supplementary table 1 for primer sequences. The *ZFP36L1* and *ZFP36L2* coding sequences, generated by PCR from the constructs, above were cloned into the MIGRI retroviral vector using the BglII and EcoRI sites. The mouse *Notch1* 3'UTR reporters were cloned from CHORI BAC clone RP23-306D20 into pSI-Check2 (Promega). See Supplementary table 1 for primer sequences.

Luciferase assays

293T cells were cultured in DMEM, 10% FCS, 2mM Glutamine and 100 U/ml Penicillin/Streptomycin then transfected with luciferase reporter (20 ng) plus *ZFP36L1* or *ZFP36L2* expression vector (0.3 – 2.5 ng) using the CalPhos kit (Clontech). Firefly and Renilla luciferase activity was analyzed 24 hours post transfection using the Dual-Glo luciferase reporter assay system (Promega) and analyzed on a TopCount NXT microplate luminescence counter.

EMSA

Complimentary oligonucleotides incorporating a T7 promoter and 61 nucleotides of the Notch1 3'UTR HCR were used for in vitro transcription of ³²P labelled RNA probe using the T7 Maxiscript kit (Ambion). 200 fmol of radiolabelled probe was incubated with 20 µg of lysate from transfected 293T cells for 20' at room temperature followed by incubation with 5mg/ml heparin and 50U/ml RNase T1. Protein-RNA complexes were resolved on a 4.5% acrylamide in 0.5× TBE gel then exposed to a Fuji Phosphorimager screen.

Tumor culture

Primary tumor cells were seeded onto OP9-DL1 stromal cells (provided by Dr Zuniga-Pflucker, University of Toronto) in α-MEM, 20% FCS, 2mM Glutamine and 100 U/ml Penicillin-Streptomycin. Compound-E was from Alexis Biochemicals. Retroviral supernatant was produced by transfection of Platinum-E packaging cells and titrated on 3T3 fibroblasts. Tumor cells were infected with retroviral supernatant in the presence of 5µg/ml Polybrene (Sigma) and centrifuged at 2500 rpm for 30 minutes.

In vivo Notch1 blocking experiments

Notch1 Blocking antibody was administered by intraperitoneal injection twice weekly for 3 weeks at a dose of 5mg/kg²⁶.

Statistics

Statistical analysis was performed using InStat-3 software (GraphPad, San Diego, CA). Tests used were Mann-Whitney and ANOVA with post-hoc analysis by Tukey.

Sequencing

Sequencing of Notch1 was performed as described²⁵.

Array CGH analysis

Leukemic DNA and cryopreserved lymphoblast samples were provided by collaborating institutions in the US [Eastern Cooperative Oncology Group (ECOG) and Pediatric Oncology Group (POG)]. All samples were collected in clinical trials with informed consent and under the supervision of local IRB committees. Consent was obtained from all patients at trial entry according to the Declaration of Helsinki. T-cell phenotype was confirmed by flow cytometry. Array-CGH analysis of human T-ALLs was performed with SurePrint G3 Human CGH 1×1M Oligo Microarrays (Agilent Technologies) according to the instructions of the manufacturer using a commercial normal DNA as reference (Promega). Array CGH data was analyzed with the Genomic Workbench 5.0.14 software (Agilent Technologies).

Supplementary Material

Refer to Web version on PubMed Central for supplementary material.

Acknowledgments

We thank all of our colleagues for their input during the preparation of this manuscript. D.J.H. was funded by a fellowship from Cancer Research UK and by the Addenbrooke's Charitable Trust. A.G. is supported by a MRC CASE studentship. M.T. is a Medical Research Council Senior Non-Clinical Fellow and also received funding for this work from BBSRC grant number BB/C506121/1. This work was supported by the National Institutes of Health grants R01CA120196 and R01CA129382 to A.F and the ECOG tumor bank grant U24 CA114737. A. F. is a Leukemia & Lymphoma Society Scholar. K. D. K. is a postdoctoral researcher funded by the "Fonds voor Wetenschappelijk Onderzoek-Vlaanderen" and recipient of a Belgian American Educational Foundation (BAEF) fellowship.

References

1. Georgescu C, et al. A gene regulatory network armature for T lymphocyte specification. *Proc. Natl. Acad. Sci. U. S. A* 2008;105:20100–20105. [PubMed: 19104054]
2. Rothenberg EV. Negotiation of the T lineage fate decision by transcription-factor interplay and microenvironmental signals. *Immunity* 2007;26:690–702. [PubMed: 17582342]
3. Rothenberg EV, Moore JE, Yui MA. Launching the T-cell-lineage developmental programme. *Nat Rev Immunol* 2008;8:9–21. [PubMed: 18097446]
4. Galante PA, et al. A comprehensive in silico expression analysis of RNA binding proteins in normal and tumor tissue: Identification of potential players in tumor formation. *RNA Biol* 2009;6:426–433. [PubMed: 19458496]
5. Taylor GA, et al. A pathogenetic role for TNF alpha in the syndrome of cachexia, arthritis, and autoimmunity resulting from tristetraprolin (TTP) deficiency. *Immunity* 1996;4:445–454. [PubMed: 8630730]
6. Carballo E, Lai WS, Blakeshear PJ. Feedback inhibition of macrophage tumor necrosis factor-alpha production by tristetraprolin. *Science* 1998;281:1001–1005. [PubMed: 9703499]
7. Bell SE, et al. The RNA binding protein Zfp3611 is required for normal vascularisation and post-transcriptionally regulates VEGF expression. *Dev. Dyn* 2006;235:3144–3155. [PubMed: 17013884]
8. Stumpo DJ, et al. Chorioallantoic fusion defects and embryonic lethality resulting from disruption of Zfp36L1, a gene encoding a CCCH tandem zinc finger protein of the Tristetraprolin family. *Mol. Cell. Biol* 2004;24:6445–6455. [PubMed: 15226444]
9. Stumpo DJ, et al. Targeted disruption of Zfp3612, encoding a CCCH tandem zinc finger RNA-binding protein, results in defective hematopoiesis. *Blood* 2009;114:2401–2410. [PubMed: 19633199]
10. Blakeshear PJ, et al. Characteristics of the interaction of a synthetic human tristetraprolin tandem zinc finger peptide with AU-rich element-containing RNA substrates. *J. Biol. Chem* 2003;278:19947–19955. [PubMed: 12639954]
11. Hudson BP, Martinez-Yamout MA, Dyson HJ, Wright PE. Recognition of the mRNA AU-rich element by the zinc finger domain of TIS11d. *Nat Struct Mol Biol* 2004;11:257–264. [PubMed: 14981510]
12. Emmons J, et al. Identification of TTP mRNA targets in human dendritic cells reveals TTP as a critical regulator of dendritic cell maturation. *RNA* 2008;14:888–902. [PubMed: 18367721]
13. Klein U, et al. The DLEU2/miR-15a/16-1 cluster controls B cell proliferation and its deletion leads to chronic lymphocytic leukemia. *Cancer Cell* 2010;17:28–40. [PubMed: 20060366]
14. Mayr C, Bartel DP. Widespread shortening of 3'UTRs by alternative cleavage and polyadenylation activates oncogenes in cancer cells. *Cell* 2009;138:673–684. [PubMed: 19703394]
15. Wiestner A, et al. Point mutations and genomic deletions in CCND1 create stable truncated cyclin D1 mRNAs that are associated with increased proliferation rate and shorter survival. *Blood* 2007;109:4599–4606. [PubMed: 17299095]
16. Sandberg R, Neilson JR, Sarma A, Sharp PA, Burge CB. Proliferating cells express mRNAs with shortened 3' untranslated regions and fewer microRNA target sites. *Science* 2008;320:1643–1647. [PubMed: 18566288]
17. Brennan SE, et al. The mRNA-destabilizing protein tristetraprolin is suppressed in many cancers, altering tumorigenic phenotypes and patient prognosis. *Cancer Res* 2009;69:5168–5176. [PubMed: 19491267]

18. Jackson RS 2nd, Cho YJ, Liang P. TIS11D is a candidate pro-apoptotic p53 target gene. *Cell Cycle* 2006;5:2889–2893. [PubMed: 17172869]
19. Baou M, et al. Involvement of Tis11b, an AU-rich binding protein, in induction of apoptosis by rituximab in B cell chronic lymphocytic leukemia cells. *Leukemia* 2009;23:986–989. [PubMed: 19092855]
20. Benjamin D, Moroni C. mRNA stability and cancer: an emerging link? *Expert Opin Biol Ther* 2007;7:1515–1529. [PubMed: 17916044]
21. de Boer J, et al. Transgenic mice with hematopoietic and lymphoid specific expression of Cre. *Eur. J. Immunol* 2003;33:314–325. [PubMed: 12548562]
22. Dumont C, et al. Rac GTPases play critical roles in early T-cell development. *Blood* 2009;113:3990–3998. [PubMed: 19088377]
23. Kelly AP, et al. Notch-induced T cell development requires phosphoinositide-dependent kinase 1. *EMBO J* 2007;26:3441–3450. [PubMed: 17599070]
24. Demarest RM, Ratti F, Capobianco AJ. It's T-ALL about Notch. *Oncogene* 2008;27:5082–5091. [PubMed: 18758476]
25. O'Neil J, et al. Activating Notch1 mutations in mouse models of T-ALL. *Blood* 2006;107:781–785. [PubMed: 16166587]
26. Wu Y, et al. Therapeutic antibody targeting of individual Notch receptors. *Nature* 2010;464:1052–1057. [PubMed: 20393564]
27. O'Connell RM, Rao DS, Chaudhuri AA, Baltimore D. Physiological and pathological roles for microRNAs in the immune system. *Nat Rev Immunol* 2010;10:111–122. [PubMed: 20098459]
28. Papadaki O, et al. Control of thymic T cell maturation, deletion and egress by the RNA-binding protein HuR. *J. Immunol* 2009;182:6779–6788. [PubMed: 19454673]
29. Winandy S, Wu L, Wang JH, Georgopoulos K. Pre-T cell receptor (TCR) and TCR-controlled checkpoints in T cell differentiation are set by Ikaros. *J. Exp. Med* 1999;190:1039–1048. [PubMed: 10523602]
30. Michie AM, Zuniga-Pflucker JC. Regulation of thymocyte differentiation: pre-TCR signals and beta-selection. *Semin. Immunol* 2002;14:311–323. [PubMed: 12220932]
31. Michie AM, et al. Constitutive Notch signalling promotes CD4 CD8 thymocyte differentiation in the absence of the pre-TCR complex, by mimicking pre-TCR signals. *Int. Immunol* 2007;19:1421–1430. [PubMed: 17981791]
32. Campese AF, et al. Notch1-dependent lymphomagenesis is assisted by but does not essentially require pre-TCR signaling. *Blood* 2006;108:305–310. [PubMed: 16507772]
33. Ciofani M, Zuniga-Pflucker JC. Notch promotes survival of pre-T cells at the beta-selection checkpoint by regulating cellular metabolism. *Nat Immunol* 2005;6:881–888. [PubMed: 16056227]
34. Pear WS, et al. Exclusive development of T cell neoplasms in mice transplanted with bone marrow expressing activated Notch alleles. *J. Exp. Med* 1996;183:2283–2291. [PubMed: 8642337]
35. Aster JC, Pear WS, Blacklow SC. Notch signaling in leukemia. *Annu Rev Pathol* 2008;3:587–613. [PubMed: 18039126]
36. Li X, Gounari F, Protopopov A, Khazaie K, von Boehmer H. Oncogenesis of T-ALL and nonmalignant consequences of overexpressing intracellular NOTCH1. *J. Exp. Med* 2008;205:2851–2861. [PubMed: 18981238]
37. Gonsalves FC, Weisblat DA. MAPK regulation of maternal and zygotic Notch transcript stability in early development. *Proc. Natl. Acad. Sci. U. S. A* 2007;104:531–536. [PubMed: 17202257]
38. Washburn T, et al. Notch activity influences the alphabeta versus gammadelta T cell lineage decision. *Cell* 1997;88:833–843. [PubMed: 9118226]
39. Keene JD. RNA regulons: coordination of post-transcriptional events. *Nat Rev Genet* 2007;8:533–543. [PubMed: 17572691]
40. Moellering RE, et al. Direct inhibition of the NOTCH transcription factor complex. *Nature* 2009;462:182–188. [PubMed: 19907488]
41. Schmidlin M, et al. The ARE-dependent mRNA-destabilizing activity of BRF1 is regulated by protein kinase B. *EMBO J* 2004;23:4760–4769. [PubMed: 15538381]

42. Benjamin D, Schmidlin M, Min L, Gross B, Moroni C. BRF1 protein turnover and mRNA decay activity are regulated by protein kinase B at the same phosphorylation sites. *Mol. Cell. Biol* 2006;26:9497–9507. [PubMed: 17030608]
43. Maitra S, et al. The AU-rich element mRNA decay-promoting activity of BRF1 is regulated by mitogen-activated protein kinase-activated protein kinase 2. *RNA* 2008;14:950–959. [PubMed: 18326031]
44. Palomero T, et al. Mutational loss of PTEN induces resistance to NOTCH1 inhibition in T-cell leukemia. *Nat. Med* 2007;13:1203–1210. [PubMed: 17873882]
45. Palomero T, Dominguez M, Ferrando AA. The role of the PTEN/AKT Pathway in NOTCH1-induced leukemia. *Cell Cycle* 2008;7:965–970. [PubMed: 18414037]
46. Weng AP, et al. Activating mutations of NOTCH1 in human T cell acute lymphoblastic leukemia. *Science* 2004;306:269–271. [PubMed: 15472075]
47. Rodriguez CI, et al. High-efficiency deleter mice show that FLPe is an alternative to CreloxP. *Nat. Genet* 2000;25:139–140. [PubMed: 10835623]
48. Fiorini E, et al. Dynamic regulation of notch 1 and notch 2 surface expression during T cell development and activation revealed by novel monoclonal antibodies. *J. Immunol* 2009;183:7212–7222. [PubMed: 19915064]
49. Dumortier A, et al. Notch activation is an early and critical event during T-Cell leukemogenesis in Ikaros-deficient mice. *Mol. Cell. Biol* 2006;26:209–220. [PubMed: 16354692]

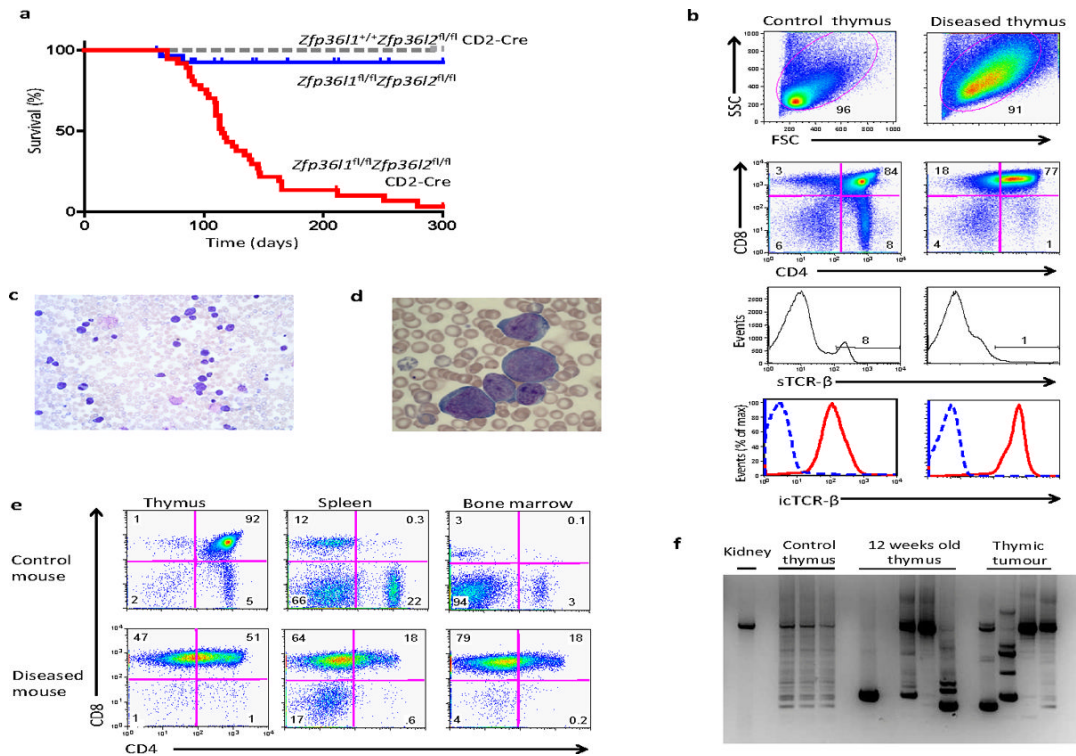


Figure 1. *Zfp361l-Zfp3612* dKO mice develop T-ALL

A. Kaplan Meier Survival of dKO (red line, n=37), *Zfp3612* single knockout (dashed line, n=14) and control (blue line, n=30) mice. B. Flow cytometric analysis of control thymus and a dKO thymic tumor stained with indicated antibodies. sTCR-β = surface TCR-β, icTCR-β = intracellular TCR-β. Solid red line = icTCR-β, broken blue line = isotype control. C. Low power examination of peripheral blood from diseased dKO mouse showing leukocytosis. D. High power examination of peripheral blood from diseased dKO mouse showing circulating lymphoblasts. E. Flow cytometric analysis of thymus, spleen and marrow from a representative control and a diseased dKO mouse. F. Dβ2-Jβ2 rearrangement by PCR of DNA from control kidney, three control thymi, five dKO thymi (12-weeks old) and four dKO thymic tumors.

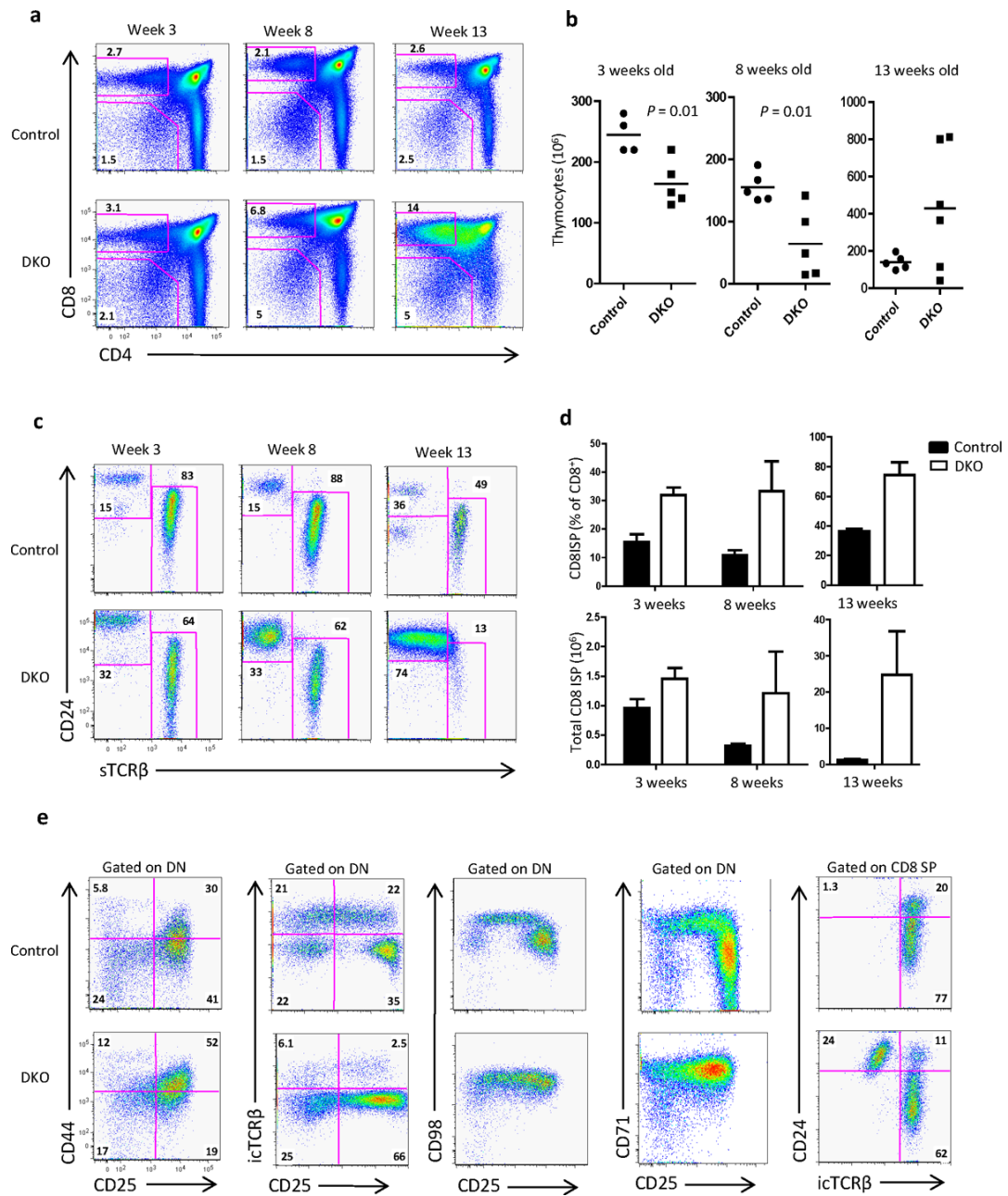


Figure 2. Thymocyte development is perturbed prior to tumor development

A. Flow cytometric plots gated on cells negative for dump channel (B220, Ter119, NK1.1, $\gamma\delta$ -TCR, Mac-1, Gr1). B. Total thymic cellularity showing thymic atrophy in dKO mice. Statistical analysis used Mann-Whitney test. C. Flow cytometric plots gated on CD8 single positive population ($CD8^+CD4^-$ as shown in A) showing proportions of immature ($CD24^{hi}sTCR\beta^-$) and mature ($CD24^{int}sTCR\beta^+$) CD8 single positive thymocytes. D. Immature CD8 single positive thymocytes as a percentage of all CD8 SP cells (upper) or absolute number per thymus (lower) at the indicated age of mice. Graphs show the mean and SEM for five mice per genotype. E. Flow cytometric plots from 3-week old mice gated on dump channel negative, $CD4^-CD8^-$ double negative thymocytes. For all flow cytometric plots numbers show the percentage of cells within the indicated gate and represent the mean from one experiment of 4–5 mice per genotype. All plots are representative of at least nine individual mice.

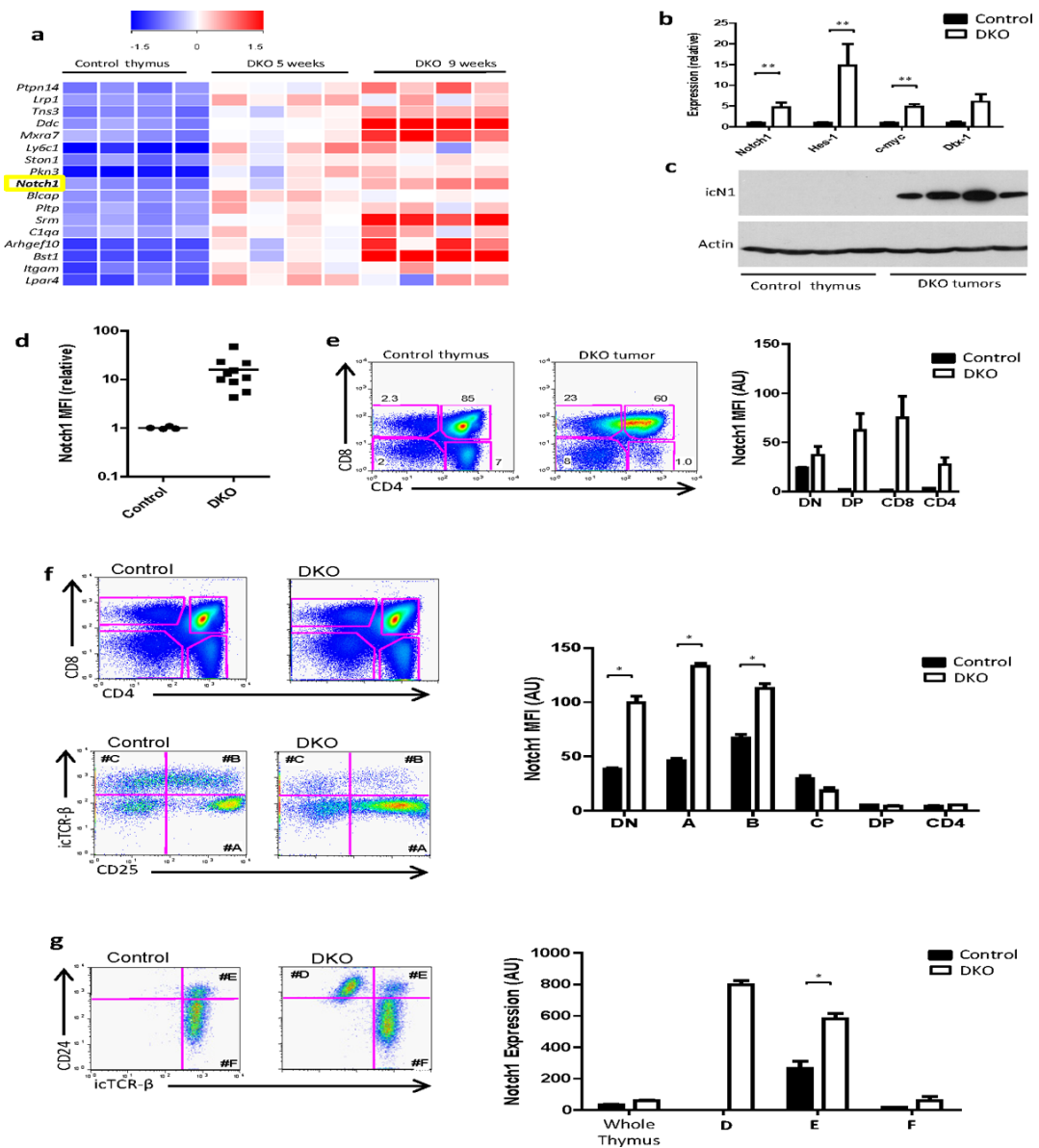


Figure 3. Expression of Notch1 is elevated in *Zfp3611-Zfp3612* dKO mice

A. Heatmap summary of microarray performed on cDNA from whole thymus of control and dKO mice at five and nine weeks of age. Criteria for inclusion are genes changing significantly ($p < 0.05$), elevated > 1.5 fold in dKO mice at both five weeks and nine weeks relative to control thymus. B. Real-time PCR performed upon cDNA from whole thymus for *Notch1* and *Notch* target genes. Values are normalised to expression of *B2m* and presented relative to expression of each gene in thymocytes from control mice. Graphs show mean and SEM of 3–8 mice. C. Immunoblot for the cleaved intracellular Notch1 (icN1) performed on whole thymus from control or diseased double knockout mice. D. Notch1 mean fluorescence intensity (MFI) by flow cytometry (normalised to isotype control) in control thymus and dKO thymic tumors. E. Notch1 expression in double negative, double positive, CD8 and CD4 populations using the gating strategy shown. Mean and SEM are shown for five separate thymic tumors. F. Notch1 expression by flow cytometry on thymocyte populations gated as shown in 3-week old. Upper plots are gated on dump channel (B220, Ter119, NK1.1, $\gamma\delta$ -TCR, Mac-1, Gr1) negative. Lower plots gated on dump⁻CD4⁻CD8⁻ DN thymocytes and show the gating of populations A, B &

C. G. Notch1 expression by flow cytometry in CD8 subpopulations (D, E & F) from 3-week old mice using gating strategy indicated. Unless stated, error bars show the mean and standard error of four-five mice per genotype. Statistical analysis performed using Mann Whitney test. (* $P < 0.05$, ** $P < 0.01$)

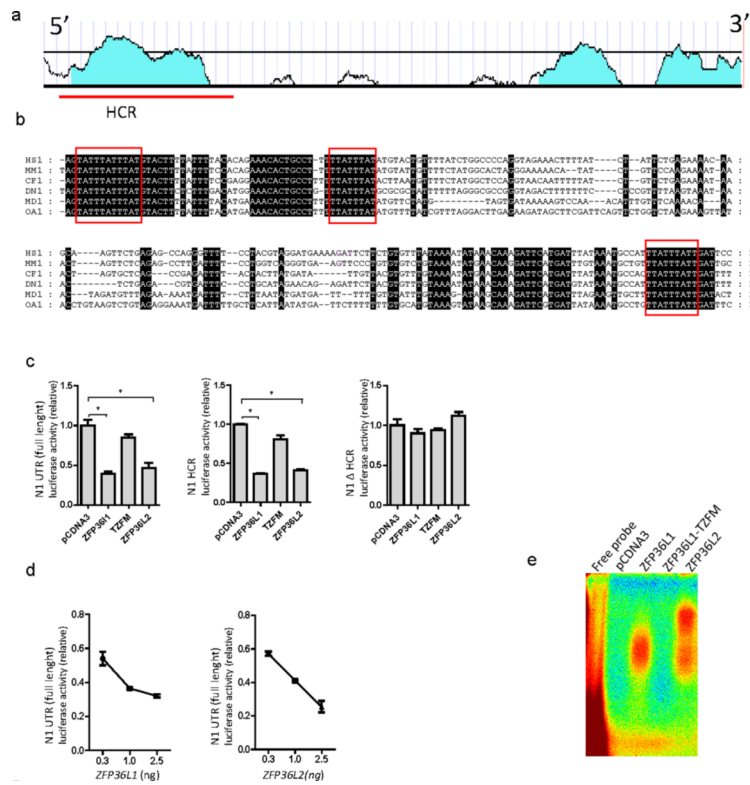


Figure 4. ZFP36L1 and ZFP36L2 exert suppression via interaction with sequences in the Notch1 3'UTR

A. *Notch1* 3'UTR presented as degree of conservation between human and mouse using the Vista Genome Browser. The highly conserved region (HCR) of interest is underlined in red. **B.** Detailed view showing inter-species sequence conservation for the underlined region in A. Black background indicates 100% conservation between human, mouse, dog, armadillo, opossum and platypus. Predicted ZFP36L1 and ZFP36L2 binding sites are boxed in red. **C.** Luciferase reporters were constructed corresponding to the full length *Notch1* 3'UTR (N1 UTR full length), the proximal HCR underlined in red in A (N1 HCR), or the *Notch1* 3'UTR with the HCR removed (N1 Δ HCR). These reporters were co-transfected into HEK293T cells along with a pCDNA3 empty control vector or pCDNA3 expressing *ZFP36L1*, *ZFP36L2* or a tandem zinc finger mutant of *ZFP36L1* (TZFM). Results are shown as the mean and SEM of five separate transfections and are representative of three experiments. Statistical analysis performed by ANOVA with Tukey post-hoc analysis (* $P < 0.001$) **D.** Titration of transfected *ZFP36L1* or *ZFP36L2*. Mean and SEM of five separate transfections are shown. **E.** Electromobility shift assay (EMSA) following incubation of a radiolabelled *Notch1* probe (corresponding to the 61 nucleotides containing the nonameric AU sequence) with lysates from 293T cells transfected with the indicated expression constructs. pCDNA3 = empty control vector, TZFM = tandem zinc finger mutant.

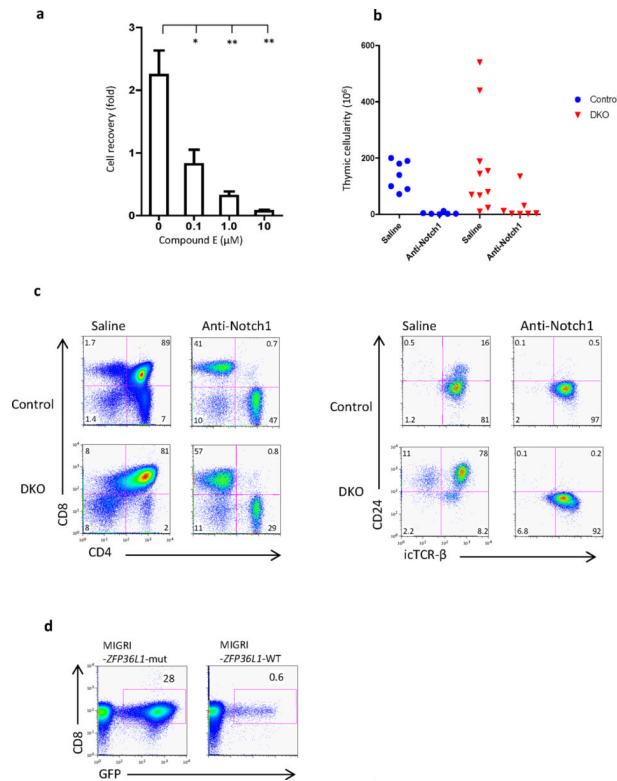


Figure 5. Inhibition of Notch or re-expression of ZFP36L1 is toxic to tumor growth

A. Primary dKO tumor cells were cultured on OP9-DL1 stromal cells for three days in the presence of increasing concentrations of the gamma-secretase inhibitor Compound E. Graph shows mean and SEM for six tumors presented relative to the number of cells seeded. Statistical analysis was performed by repeated measures ANOVA with Tukey post hoc analysis. (** $p < 0.01$, *** $p < 0.001$) **B.** Notch1 blocking antibody, or saline control, was administered *in vivo* to 11 week old control and dKO mice. After three weeks of treatment thymus was analysed by flow cytometry. Post-treatment thymic cellularity is shown for individual mice. **C.** Representative flow cytometry plots of thymus after treatment with control or Notch1 blocking antibody. CD4–8 plots are gated on thymocytes negative for B220, NK1.1, $\gamma\delta$ -TCR, mac-1, Gr1, Ter119. CD24-icTCR- β plots are gated on the CD8 single positive quadrant. **D.** Primary thymic tumors from dKO mice were cultured on OP9-DL1 stromal cells for 24 hours before infection with equivalent titres of retrovirus expressing either ZFP36L1 or the tandem zinc finger mutant of ZFP36L1 (TZFM). After three days cells were analysed by flow cytometry. Flow cytometry plots shown are representative of infection of five separate dKO tumors.